

## Shaking table model study on the dynamic response of reinforced soil walls

R.J. BATHURST & M.M. EL-EMAM, GeoEngineering Center at Queen's-RMC, Geotechnical Group, RMC, Kingston, Ontario, Canada.

M.M. MASHHOUR, Head, Structural Engineering Dept, Zagazig University, Zagazig, Sharkia, Egypt.

**ABSTRACT:** A series of reduced-scale shaking table experimental tests were performed at the Royal Military College of Canada (RMC) to assess the seismic performance of reinforced soil walls constructed with different toe boundary conditions. The experimental results show that the toe boundary condition has a significant effect on the seismic response of the structure. The facing panel attracted a significant portion of the lateral earth force when the toe of the model was constrained horizontally. The vertical toe loads that developed under static and dynamic loading were found to be larger than the facing self-weight. A restrained toe was found to reduce wall lateral deformations and reinforcement loads under both static loading and simulated base excitation due to earthquake. The data gathered from this program is used to identify deficiencies in current seismic design methodologies for reinforced soil structures.

### 1 INTRODUCTION

Geosynthetic and metal strip reinforced soil walls are routinely designed using limit equilibrium analysis methods that are based on Mononobe-Okabe earth pressure theory. These methods have been based largely on the results of numerical modelling of reinforced soil structures with relatively in-extensible steel reinforcement (Bathurst & Alfaro 1996). Alternatively, variants of Newmark's sliding block method have been recommended to calculate permanent displacement of the reinforced soil zone due to base acceleration at sites with strong earthquake records (FHWA 2001, Cai & Bathurst 1996). However, neither limit equilibrium methods nor displacement methods can account for the facing panel and toe restraint as major structural elements. Experimental, numerical and field data has shown that a rigid facing panel can reduce wall lateral deformations and increase the stability of reinforced soil structures under both static loading and during base shaking due to earthquake (Tatsuoka 1993, Bathurst & Hatami 1998, Bathurst & Walters 2000).

In this paper, results of two reduced-scale reinforced soil wall models tested on a shaking table are reported. The emphasis of the paper is on the quantitative effect of the toe boundary condition (hinged or hinged and free to move horizontally) on the response of the models to simulated base excitation due to earthquake.

### 2 SHAKING TABLE TESTS

#### 2.1 Model configurations

A total of fourteen 1 m-high model walls at 1/6 scale comprise the experimental portion of the current research program. Results of two model walls from this series of tests are presented that demonstrate the influence of the facing toe restraint condition on the response of reinforced soil walls to base acceleration. Figure 1 shows a typical reinforced soil model wall with a full height panel facing. The reinforcement vertical spacing for the two models was  $S_v = 0.23$  m and the reinforcement length,  $L$ , was chosen to give  $L/H=0.6$ , where  $H$  is the height of the model (Figure 2). The model walls were designed in accordance with similitude rules proposed by Iai (1989), to ensure that the geometry of the walls, soil properties and stiffness of the geosynthetic reinforcement were typical for a prototype-scale model (i.e. field scale). In order to isolate the influence of the toe boundary condition on the model response, two different toe arrangements were used. In the first arrangement (hinged toe), the

model toe was restrained from movement in the vertical and horizontal directions, while it was free to rotate. The second arrangement (sliding toe) allowed the toe to slide horizontally and rotate, while restrained from vertical movement. The facing panels were braced externally during construction and released prior to base shaking. Additional details on the model configurations and a description of the RMC shaking table facility are reported by El-Emam et al. (2001).

#### 2.2 Testing materials

The backfill material used in the model tests was an artificial, uniformly graded sand, with angular to subangular particles. This sand was selected to ensure a repeatable soil condition (i.e. same relative density after compaction using horizontal vibration of the shaking table) for all tests. The sand had a measured unit weight of  $15.7 \text{ kN/m}^3$  at the end of construction. Direct shear tests on the sand prepared to the same unit weight gave a peak direct shear friction angle  $\phi_p = 51^\circ$ , constant volume friction angle  $\phi_{cv} = 45^\circ$ , and dilation angle  $\psi = 14.5^\circ$ . A knitted geogrid polyester product was used for the reinforcement in the current investigation. The geogrid has a linear axial stiffness,  $J = 90 \text{ kN/m}$  with a tensile yield strength of  $12 \text{ kN/m}$ . The stiffness of

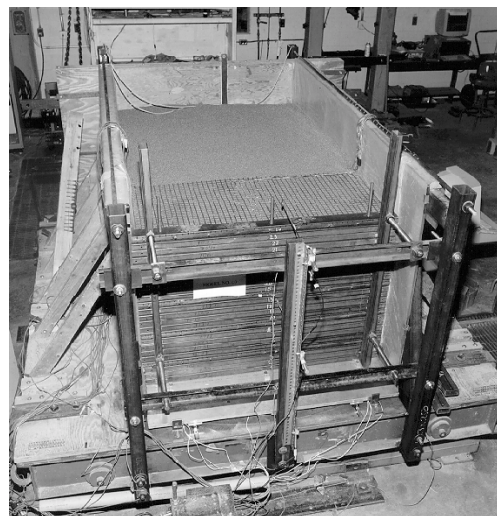


Figure 1. 1/6 scale reinforced soil retaining model wall under construction with full height panel facing.

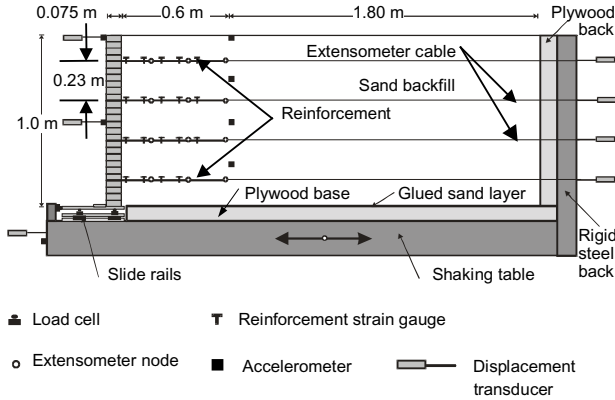


Figure 2. Example test configuration and instrumentation layout for model walls. Note: Facing constructed as continuous facing panel.

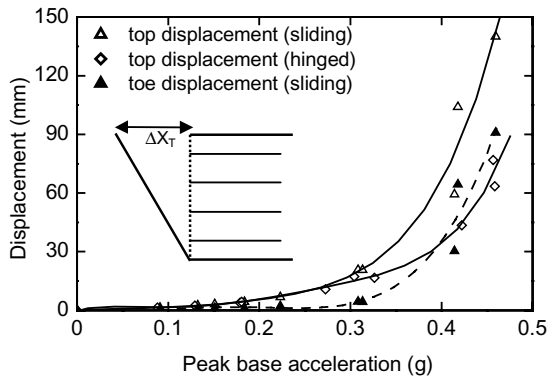


Figure 3. Displacement measured at the top and bottom of the model wall facing panels vs. peak input base acceleration amplitude.

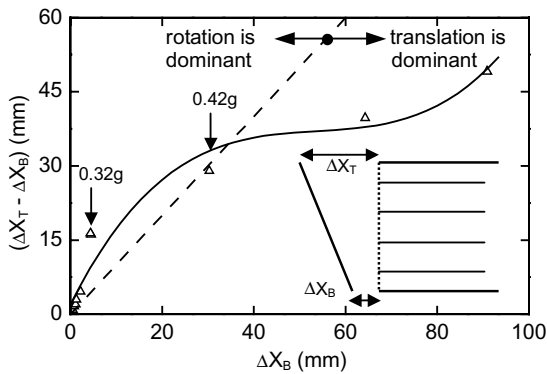


Figure 4. Facing displacement due to rotation vs. displacement due to base sliding for sliding toe model.

this geogrid in reduced-scale models is typical of reinforcement stiffness values for extensible (i.e. geosynthetic) reinforcement at prototype scale.

### 2.3 Instrumentation and base excitation

Figure 2 illustrates the test wall configuration and the instrumentation layout. A total of 64 instruments were deployed in each model wall. Facing displacements were measured using displacement transducers mounted against the facing panel. Reinforcement local strain was measured using strain gauges bonded to selected longitudinal members of each reinforcement layer. The global strains (i.e. the strains measured over several geogrid apertures) were measured using extensometers attached to the reinforcement layers at selected geogrid junctions. Accelerometers

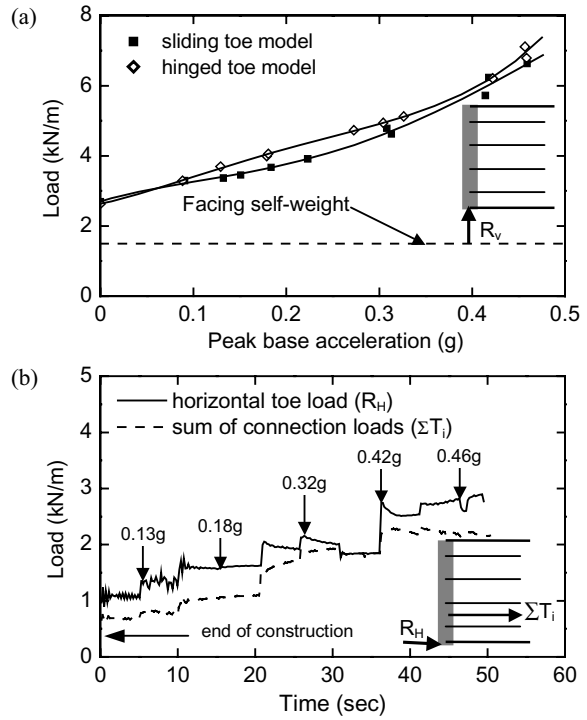


Figure 5: a) Vertical toe load vs. peak input base acceleration amplitude, and b) horizontal toe load and sum of the connection loads vs. time for hinged toe model.

were used to measure acceleration response over the height of the model wall as well as the input base acceleration during shaking. Vertical and horizontal load cells were installed beneath the facing panel to measure the forces transmitted to the footing (facing toe). Three linear roller bearings were used across the length of the facing panel to decouple the measured toe force into horizontal and vertical components.

Data from all instrumentation were collected using two data acquisition systems with sampling rates great enough to avoid aliasing and to capture peak dynamic response values. The base input motion was controlled by a stepped-amplitude sinusoidal displacement function applied at a frequency of 5 Hz. The base input motion was stepped in equivalent 0.05g increments every 5 seconds until excessive model deformation occurred.

## 3 MODEL TEST RESULTS

Maximum lateral displacements at the top and bottom of the facing panel for the model walls versus peak input base acceleration amplitude are shown in Figure 3. For the hinged toe model, the facing displacement was due only to facing rotation, while for the sliding toe model, the facing displacement was a combination of facing panel rotation and translation at the facing toe. The less-restrained model wall with the sliding toe generated greater outward movement at the top of the wall than the hinged toe model for peak base accelerations greater than 0.3g.

Figure 4 shows the relative displacement ( $\Delta X_T - \Delta X_B$ ) at the top of the wall with respect to base sliding ( $\Delta X_B$ ) for the sliding toe model. For acceleration amplitudes smaller than 0.3g, the predominant facing deformation mode is wall rotation. At peak acceleration amplitudes higher than 0.3g, base sliding becomes the dominant wall deformation mode. Taken together the facing displacement time-histories confirm that the type of toe restraint condition influences both the mode and magnitude of displacements particularly during strong base excitation.

The history of recorded vertical toe load with peak input base acceleration is shown in Figure 5a. It is seen from the figure that the vertical toe load is significantly greater than the self-weight

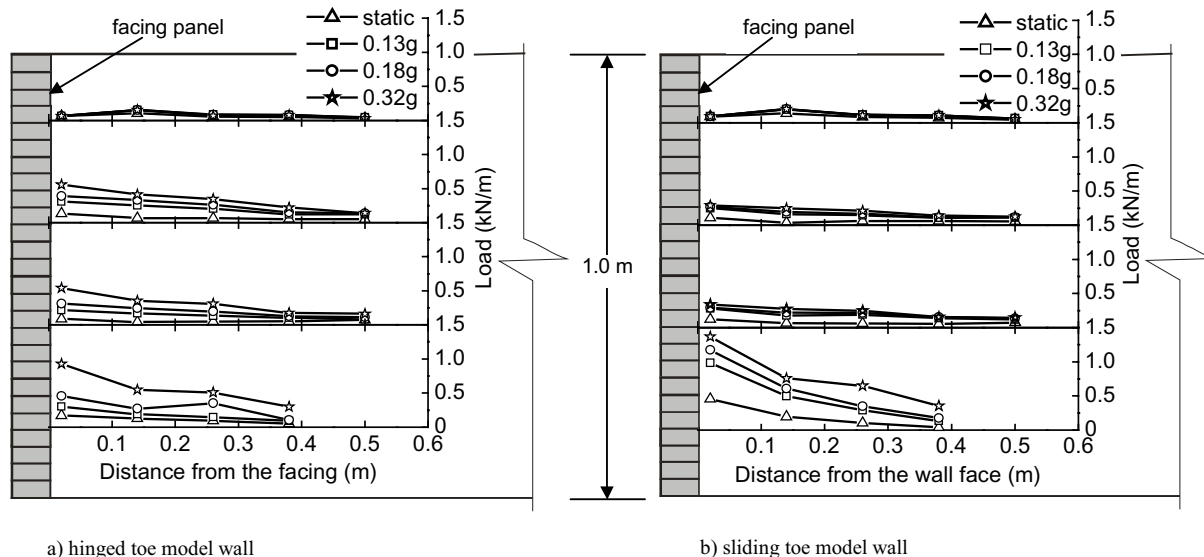


Figure 6. Variation of total reinforcement forces with distance from the facing panel at different peak input base acceleration amplitudes.

of the facing panel for both walls at end of construction (static loading) and during subsequent base excitation. This observation is attributed to vertical down-drag forces developed at the back of the facing panel due to settlement of the soil in the reinforced zone with respect to the rigid facing panel. Results of Figure 5a show that down-drag forces increase with the amplitude of base acceleration and that this response is sensibly independent of the type of toe boundary condition.

Time histories of measured horizontal toe load,  $R_H$ , and sum of total reinforcement connection loads,  $\sum T_i$ , are shown in Figure 5b. The total reinforcement load is back-calculated from measured strains in the reinforcement directly behind the facing panel and the stiffness modulus of the reinforcement. Total reinforcement load and toe load generally increase with the amplitude of peak base acceleration. The figure shows that the restrained toe attracted a significant portion of the total horizontal earth force acting against the facing panel at the end of construction (approximately 59% at release of external braces). This is not a surprising result since the toe of the model wall is very much stiffer than the reinforcement layers at the end of construction. During base excitation, soil-reinforcement interaction was mobilised and the portion of the horizontal earth force taken by the reinforcement increased. Nevertheless, the toe carried not less than 50% of the horizontal earth force recorded at the facing panel during the base excitation program.

Figure 6 shows the reinforcement load distribution along the length of each layer at different peak base acceleration values for both sliding and hinged toe models. It is clear that the reinforcement loads generally increase with depth of the layer below the backfill surface and with the distance from the free end of reinforcement. In addition, the reinforcement loads generally increase as the peak base acceleration increases. The data in the figure also shows that the reinforcement loads under static and dynamic loading are greatest at the connections for both sliding and hinged toe models. Furthermore, the largest reinforcement loads in each model wall are in the bottom-most layer. The top reinforcement layer in both models did not develop significant tensile load compared to the other layers which may be attributed to the shallow depth of overburden for this layer (i.e. 0.15 m of soil).

Figure 7 shows the magnitude and distribution of the measured connection loads at the end of construction and at selected acceleration amplitude values. For the sliding toe model, the reinforcement connection load in the bottom layer was the largest load at the end of construction and also increased significantly during base excitation. Over the range of peak acceleration values shown, the connection loads were more uniform for the

hinged toe model. The results in Figure 7 demonstrate that the toe boundary condition influences not only the magnitude of reinforcement loads but also the distribution of loads under both static and dynamic loading. Also plotted in Figure 7 are the predicted connection loads using the modified Mononabe-Okabe method with the so-called contributory area approach (Bathurst 1998), peak soil direct shear friction angle and, the assumption of fully mobilised soil-wall friction angle (i.e.  $\phi_{peak} = \delta = 51^\circ$ ). This method ignores the contribution of the restrained toe. Nevertheless, the envelope of predicted connection loads can be argued to be reasonably accurate for the middle layers of reinforcement but over-estimates the load in the top layer (possibly due to the small overburden pressures discussed earlier) and underestimates the bottom layer load for the sliding toe condition. Figure 8 compares the measured and predicted sum of the total connection loads,  $\sum T_i$ , for both model walls. The predicted values of the sum of connection loads are larger than the measured values for the hinged model which is consistent with ignoring the contribution of the toe. However, for the sliding toe model, the predicted sum of the connection loads is in generally good agreement with the measured values up to acceleration amplitude 0.3g. For peak acceleration amplitudes higher than 0.3g, the pseudo-static method over-predicted the sum of the total connection loads. The suitability of any limit-equilibrium method to predict earth forces after large displacements is likely problematic due to the accompanying large wall rotations. Coincidentally, FHWA (2001) and NCMA guidelines (Bathurst 1998) recommend that pseudo-static methods should be restricted to sites where peak ground horizontal acceleration is not expected to exceed 0.29g.

Outward (away from the soil) acceleration amplification factors plotted against input base acceleration amplitude are shown in Figure 9. It is clear from the figure that prior to an acceleration amplitude of 0.3g, all outward acceleration amplification factors are small, between 1.0 and 1.3, but increase significantly thereafter. Increasing magnitude of amplification factor with increasing base excitation for extensible reinforcement shaking table models has also been reported by Matsuo et al. (1998). In general, the outward acceleration amplification factors are larger for the model with a hinged toe than for the model with a sliding toe. This observation is in accordance with numerical results for prototype-scale propped panel walls subjected to base excitation reported by Bathurst and Hatami (1998). Figure 9 also shows that there is a phase difference between input base acceleration and response accelerations for both hinged and sliding toe model walls. Out-of-phase motions in the soil can be expected to have a

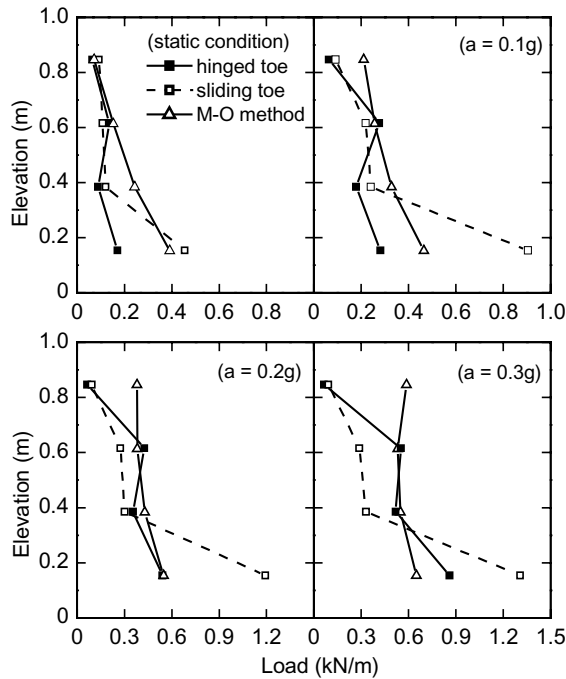


Figure 7. Measured versus predicted connection loads for sliding and hinged toe model walls at different peak input base acceleration.

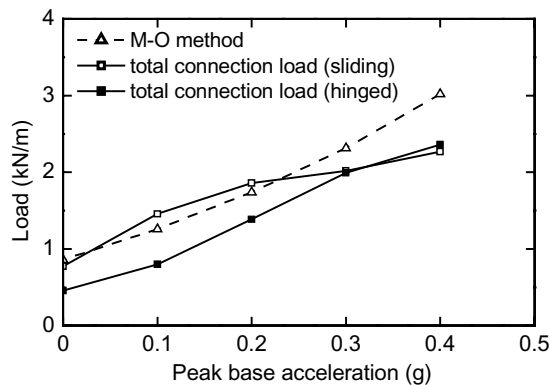


Figure 8. Measured and predicted sum of connection loads for model walls with hinged and sliding toe versus peak input base acceleration.

marked effect on the distribution of dynamic reinforcement load with time during base excitation (e.g. Steedman and Zeng 1990).

#### 4 CONCLUSIONS AND IMPLICATIONS TO DESIGN

Some important conclusions and implications to current design practice are summarised below.

A stiff facing panel with a horizontally restrained toe is a structural element that acts to reduce the magnitude of lateral wall displacements and the total load in the reinforcement layers under both static conditions and during idealised ground motions simulating earthquake loading. The hinged toe model in this study was shown to attract at least 50% of the total earth force acting on the back of the facing panel. The contribution of the toe is not considered in current limit-equilibrium based analysis and design methods for reinforced soil walls. For the unrestrained toe model, the conventional pseudo-static method gave reasonably accurate predictions of the sum of connection loads under static (end-of-construction) conditions and up to peak base acceleration amplitudes of 0.3g.

The vertical load acting at the toe of the facing was found to be greater than the self-weight of the facing panel due to down-

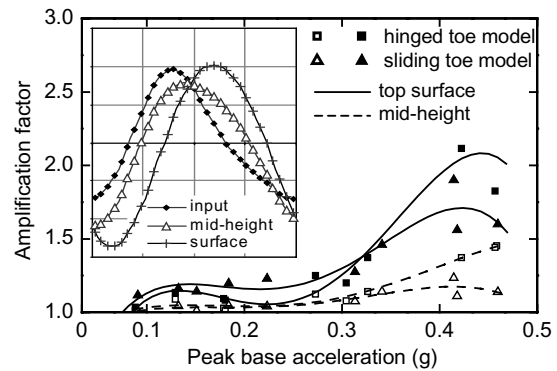


Figure 9. Amplification factors for hinged and sliding toe model walls vs. peak input base acceleration.

drag forces acting at the back of the facing panel. Downdrag forces likely contributed to the observed relatively high connection loads acting immediately behind the facing panels. These additional loads are not considered explicitly in current design codes and hence current practice may be non-conservative (unsafe) particularly during base excitation leading to wall rotations.

Input base acceleration was amplified towards the backfill surface. In a field-scale wall, ground amplification of the magnitudes experienced in these tests could lead to additional loads on the facing panels and reinforcement layers which are difficult to incorporate in current pseudo-static design methods. An important implication of this observation is that the assumption of a depth independent (constant) horizontal seismic coefficient expressed as a function of site peak ground acceleration may not be appropriate for seismic design of reinforced soil wall structures.

#### REFERENCES

- Bathurst, R.J. 1998. *NCMA Segmental Retaining Wall Seismic Design Procedure – Supplement to Design Manual for Segmental Retaining Walls* (Second Edition 1997) published by the National Concrete Masonry Association, Herndon, VA, 187 p.
- Bathurst, R.J. & Alfaro, M.C. 1996. Review of seismic design, analysis and performance of geosynthetic reinforced walls, slopes and embankments. Keynote lecture. *Proc. of Inter. Symp. on Earth Reinforcement*, Fukuoka, Kyushu, Japan, (2): 887-918.
- Bathurst, R.J. & Hatami, K. 1998. Seismic response analysis of a geosynthetic-reinforced soil retaining Wall. *Geosyn. Intern.* 5(1-2): 127-166.
- Bathurst, R.J. & Walters, D. 2000. Lessons learned from full scale testing of geosynthetic reinforced soil retaining walls. *GeoEng2000*, Melbourne, Australia, November 2000, 14 p.
- Cai, Z. & Bathurst, R.J. 1996. Seismic-induced permanent displacement of geosynthetic reinforced segmental retaining walls. *Can. Geot. J.*, (31): 937-955.
- El-Emam, M.M., Bathurst, R.J., Hatami, K. & Mashhour, M.M. 2001. Shaking table and numerical modelling of reinforced soil walls. *Proc. Inter. Symp. on Earth Reinforcement*, Fukuoka, Kyushu, Japan, (1): 329-334
- FHWA 2001. Mechanically stabilized earth walls and reinforced soil slope design and construction guidelines, *Federal Highway Administration*, Washington DC, USA.
- Iai, S. 1989. Similitude for shaking table tests on soil-structure-fluid models in 1g gravitational field. *Soils Found.* 29(1): 105-118.
- Matsuo, O., Tsutsumi, T., Yokoyama, K. & Saito, Y. 1998. Shaking table tests and analyses of geosynthetic-reinforced soil retaining walls. *Geosyn. Intern.* 5(1-2): 97-126.
- Steedman, R.S. & Zeng, X. 1990. The influence of phase on the calculation of pseudo static earth pressure on retaining walls. *Geotechnique.* 40(1): 101-112.
- Tatsuoka, F. 1993. Roles of facing in soil reinforcing. Keynote lecture. *Proc. of Inter. Symp. on Earth Reinforcement*, Fukuoka, Kyushu, Japan, (2): 831-870.